Appl. Phys. A (2016) 122:568
DOI 10.1007/s00339-016-0105-9

Applied Physics A
Materials Science & Processing

Influence of temperature on Al/p-$CuInAlSe_2$ thin-film Schottky diodes

Usha Parihar[1] · Jaymin Ray[2] · C. J. Panchal[3] · Naresh Padha[1]

Received: 17 February 2016 / Accepted: 27 April 2016

Abstract Al/p-$CuInAlSe_2$ Schottky diodes were fabricated using the optimized thin layers of $CuInAlSe_2$ semiconductor. These diodes were used to study their temperature-dependent current–voltage (I–V) and capacitance–voltage (C–V) analysis over a wide range of 233–353 K. Based on these measurements, diode parameters such as ideality factor (η), barrier height (ϕ_{bo}) and series resistance (R_s) were determined from the downward curvature of I–V characteristics using Cheung and Cheung method. The extracted parameters were found to be strongly temperature dependent; ϕ_{bo} increases, while η and R_s decrease with increasing temperature. This behavior of ϕ_{bo} and η with change in temperature has been explained on the basis of barrier inhomogeneities over the MS interface by assuming a Gaussian distribution (GD) of the ϕ_{bo} at the interface. GD of barrier height (BH) was confirmed from apparent BH (ϕ_{ap}) versus $q/2kT$ plot, and the values of the mean BH and standard deviation (σ_s) obtained from this plot at zero bias were found to be 1.02 and 0.14 eV, respectively. Also, a modified $\ln(J_s/T^2) - q^2\sigma_s^2/2k^2T^2$ versus q/kT plot for Al/p-$CuInAlSe_2$ Schottky diodes according to the GD gives ϕ_{bo} and Richardson constant (A^{**}) as 1.01 eV and 26 $Acm^{-2}\,K^{-2}$, respectively. The Richardson constant value of 26 $Acm^{-2}\,K^{-2}$ is very close to the theoretical value of 30 $Acm^{-2}\,K^{-2}$. The discrepancy between BHs obtained from I–V and C–V measurements has also been interpreted.

✉ Jaymin Ray
jayminray@gmail.com

[1] Department of Physics and Electronics, University of Jammu, Jammu, J&K, India

[2] Department of Physics, Indian Institute Teacher Education, Gandhinagar, Gujarat, India

[3] Applied Physics Department, The M.S. University of Baroda, Vadodara, Gujarat, India

1 Introduction

$Cu(In,Al)Se_2$ (CIAS) is a direct bandgap quaternary semiconductor, with bandgap varying between 1.0 eV (CIS) to 2.7 eV ($CuAlSe_2$) by Al addition, and has been found to be a potential candidate for low-cost solar cells [1]. Further, there are two main families of possible photovoltaic devices in the form of metal-to-semiconductor Schottky and semiconductor–semiconductor of homo-/hetero-junction variety. The later can be made via the same semiconductor through different types of doping, yielding relatively more complex structure compared to MS Schottky junction [2, 3].

Moreover, metal–semiconductor structures are important research tools for the characterization of new semiconductor materials and simultaneously play a vital role in constructing some useful devices [4, 5]. The electrical properties of the Schottky contacts depend on the density of interface states, and therefore, the control of interface quality has been found promising for device performance, stability and reliability [6]. The current–voltage (I–V) characteristics of the Schottky diode measured at room temperature do not provide satisfactory information about the conduction process and the nature of barrier at the metal–semiconductor (MS) interface, whereas the temperature-dependent I–V characteristics allow us to understand the different aspects of the conduction mechanisms. Thermionic emission (TE) current transport mechanism has widely been used to extract the Schottky diode parameters; however, several anomalies have been reported at both low and high temperatures [7–12]. Further, it has

Published online: 04 May 2016

been found that BH (ϕ_{bo}) increases and ideality factor (η) decreases with increasing temperature [13–16]. Various models have been used to explain these deviations. Some authors suggest 'inhomogeneities at a real MS interface' be the cause of the anomalous behavior [8–12]. Further, the same authors suggest that the temperature dependence of BHs and ideality factors can be successfully explained on the basis of TE coupled with GD of BHs. The ballistic electron emission microscopy (BEEM) has also supported the existence of a GD of the BHs in Schottky diodes [16]. In addition, we could say the study of the absorber layer in Schottky diode application to explore the capability of the material to be used in other optoelectronics devices. Regarding the photovoltaic devices, one could try for by taking the thinner aluminum contact in order to use it as a Schottky solar cell.

In this paper in addition to the temperature-dependent I–V, C–V measurements, in the temperature range 233–353 K, of Al/p-$CuInAlSe_2$ Schottky diodes are reported and studied. The temperature dependence of BHs and ideality factors has been interpreted on the basis of existence of GD of the BHs around a mean value.

2 Experimental details

Polycrystalline chalcopyrite composition $CuIn_{1-x}Al_xSe_2$ (CIAS) with $x = 0.19$ was prepared by using melt-quenching method as described earlier [17]. Thin films of this material were then deposited on organically cleaned glass substrate under varying substrate temperatures and film thicknesses by using flash evaporation techniques [17]. In order to prepare Al/p-$CuInAlSe_2$ Schottky diodes, initially silver was deposited over organically cleaned glass substrate which was followed by the flash deposition of 700 nm thick annealed CIAS layer. The annealing for this purpose was performed at 573 K for the duration of 1 h in a vacuum chamber at a base pressure of 10^{-2} mbar. Finally, circular Schottky diodes of area 6×10^{-3} cm^2 were formed by thermally depositing aluminum over the optimized CIAS layer. The rate of deposition of all the metals was kept at 0.5–0.6 nm s^{-1}, whereas rate of 0.3–0.4 nm s^{-1} was maintained for CIAS deposition at a base pressure of 2×10^{-6} mbar. The prepared diodes were then tested for the temperature-dependent (233–353 K) I–V as well as capacitance–voltage (C–V) behavior using computer-interfaced I–V/C–V setup comprising of a programmable source meter (Keithley make, model 2400), precision programmable LCR meter (Agilent make, model 4284A), Hot plate, thermocouple, cryogenic setup (Lake Shore make, model Cryodyne 22CP CTI) equipped with compressor (model 8200 CTI) and temperature controller (Lake Shore make, model 321). The interfacing of these instruments was established by using LabVIEW software by National Instruments, USA.

3 Results and discussion

3.1 Current–voltage–temperature analysis

The temperature-dependent I–V characteristics of Al/p-$CuIn_{0.81}Al_{0.19}Se_2$ Schottky diodes of the area of 6×10^{-3} cm^2 in the temperature range from 233 to 353 K are shown in Fig. 1. The reverse characteristics of the diode demonstrate nonsaturating response with bias as shown in Fig. 1. The behavior may be explained on the basis of the spatial inhomogeneity of BH [11]. For inhomogeneous MS contacts, the reverse characteristics may be dominated by the current which flow through the low-BH patches. The semilogarithmic forward I–V curves as shown in Fig. 1 have also been found nonlinear in nature; the nonlinearity in the I–V characteristics is a complex feature which arises due to several factors when a number of noninteracting parallel diodes with a GD of BHs act simultaneously, and thus is not preferred for the extraction of barrier parameters [18]. However, the linear range of the forward I–V plot in the undertaken diodes is short; therefore, the determination of the diode parameters using it is not possible. Thus, an alternative approach developed by Cheung and Cheung [19] in the light of Eqs. (1) and (2) has been used to extract Schottky diode parameters corresponding to downward curvature of temperature-dependent forward I–V plots (Fig. 1). The ideality factors (η), BHs (ϕ_{bo}) and series resistances (R_s) as measured on the basis of Eqs. (1) and (2) are presented in Table 1.

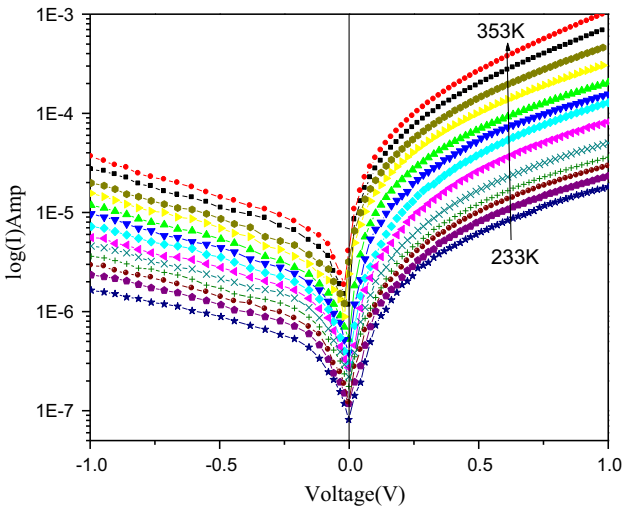

Fig. 1 log(I) versus V characteristics of Al/p-$CuIn_{0.81}Al_{0.19}Se_2$ Schottky diode

Table 1 Diode parameters extracted from temperature-dependent I–V characteristics by Cheung's method

Temp. (K)	Ideality factor (η)	Barrier height ϕ_{IV} (eV)	Barrier height ϕ_{CV} (eV)	Series resistance R_s (kΩ)	Acceptor density of states × 10^{19} N_A (cm^{-3})
233	6.40	0.46	0.81	36	0.97
243	4.15	0.49	0.79	31	1.02
253	3.10	0.52	0.78	29	1.08
263	2.53	0.54	0.76	25	1.09
273	2.26	0.56	0.74	21	1.13
283	2.02	0.57	0.73	14	1.17
293	1.76	0.59	0.71	10	1.23
303	1.64	0.60	0.68	7	1.44
318	1.54	0.61	0.67	5	1.74
323	1.41	0.62	0.66	4	1.76
333	1.28	0.64	0.65	3	1.83
343	1.18	0.64	0.63	2	1.93
353	1.13	0.65	0.62	1	2.01

$$\frac{d(V)}{d(\ln J)} = R_s AJ + \frac{\eta}{\beta} \quad (1)$$

$$H(J) = R_s AJ + \eta\phi_{bo} \quad (2)$$

As shown in Table 1, the values of ϕ_{bo} for the Al/p-$CuIn_{0.81}Al_{0.19}Se_2$ Schottky diodes vary significantly from 0.46 to 0.65 eV, while η changes from 6.40 to 1.13 for the temperature range from 233 to 353 K. Such high value of ideality factor at 233 K, compare to the 353 K, is may be due to the interface roughness, interfacial reactions, diffusion/interdiffusion of the contaminations of applied materials on semiconductor surface, inhomogeneities of thickness and composition of the layer and nonuniformity of interfacial charges or the presence of a thin insulating layer, because of trace quantities of oxygen, between the metal and the semiconductor [20]. Figure 2 shows the graphical representation of experimental value of ϕ_{bo}, η as in the temperature of 233–353 K.

Since current transport across the metal–semiconductor interface is a temperature-activated process, electrons at low temperature pass over the lower barriers and the current is dominated by diodes with lower SBH and a larger ideality factor. In other words, as the temperature increases, more and more electrons have sufficient energy to overcome the higher barrier; thus, the dominant BH will increase with the temperature [21, 22]. Further, the higher values of the ideality factor ($\eta > 1$) indicate deviation of the current mechanism from TE theory. Idealities greater than one can also be attributed to the presence of a thick interfacial insulator layer between the metal and semiconductor [1, 23].

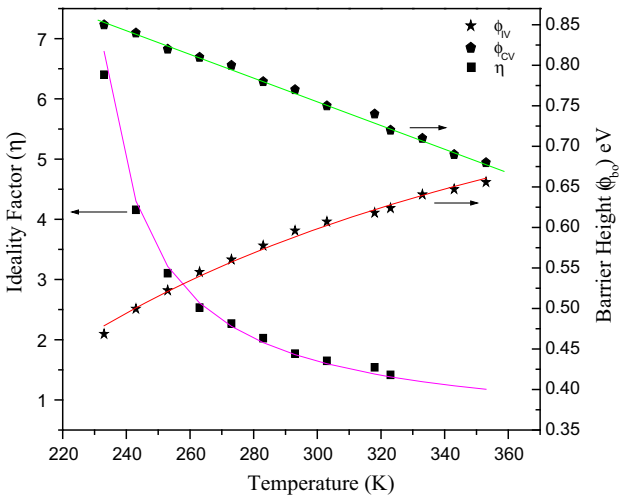

Fig. 2 Barrier height (ϕ_{CV}) obtained from C–V data and zero-bias barrier height (ϕ_{IV}) as well as the ideality factor (η) for the Al/p-$CuInAlSe_2$ Schottky diodes obtained from the forward bias I–V data at various temperatures

Moreover, the variation of series resistance with temperature can be seen from Table 1 which depicts a decrease in its value with increase in temperature; the change is more predominant at low temperatures in comparison with high temperatures. Such behavior of series resistance variation has been ascribed to the particular distribution of the interface states. In the case of metal–semiconductor interface as explained above, the electrons at low temperature pass over the lower barriers and therefore current will flow through patches of the lower Schottky BH and results in a larger ideality factor and hence higher series resistance [24].

3.2 Richardson plots

Thermionic emission theory is normally used to extract the SBD parameters. However, there have been several reports about the deviation of these parameters from this classical TE theory [8, 25]. One can also evaluate the BH by using the Richardson plot of the saturation current as follows,

$$\ln\left(\frac{J_s}{T^2}\right) = \ln(A^{**}) - \frac{q\phi_{bo}}{KT} \tag{3}$$

According to Eq. (3), the plot of ln (J_s/T^2) versus 1000/T provides a straight line with slope giving the activation energy and intercept at the ordinate yielding the effective Richardson constant (A^{**}). However, the plot of ln (J_s/T^2) versus 1000/T of the experimental data has been found deviating from linearity below 293 K (refer Fig. 3).

The nonlinearity may be explained on the basis of temperature dependence of η and ϕ_{bo} as been reported by several authors [14–16]. The experimental data fit asymptotically with a straight line, yielding Richardson constant (A^{**}) value of 2.14 × 10^{-4} Acm^{-2} K^{-2}. This value of A^{**} is lower than the reported A^{**} (=30 Acm^{-2} K^{-2}) value of CIS. The deviation in the Richardson plot as well as A^{**} value may be due to image force lowering, tunneling current, recombination in the space charge region appearing at low voltage and variation of the charge distribution near the interface [26]. According to Horvath [7], the A^{**} value obtained from the temperature-dependent I–V characteristics may be affected by the lateral inhomogeneity of the barrier and the fact that it is different from the theoretical value may be connected to real effective mass which is different from that of the calculated one.

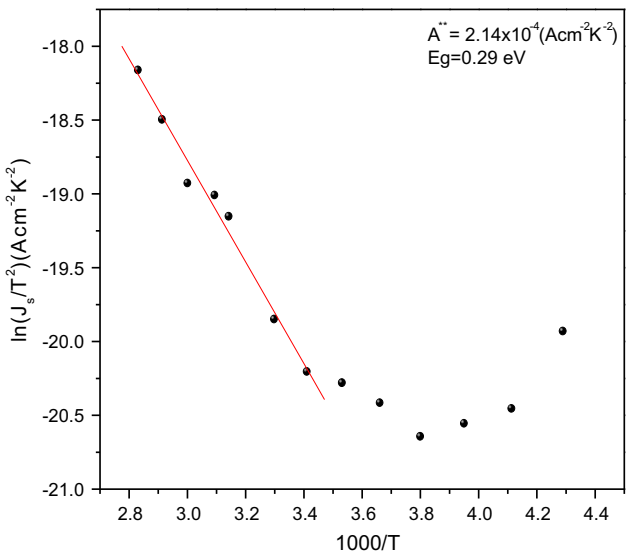

Fig. 3 Richardson plot of ln(J_s/T^2) versus 1000/T for Al/p-$CuInAlSe_2$ SBD

3.3 Barrier height inhomogeneities

Barrier height inhomogeneity model is based on an assumption that there are large number of parallel diodes having different SBD's, and every SBD can independently make contribution to the current so that the total current across the diode is sum of the current flowing in individual diodes with different areas; however, the apparent BH (ϕ_{ap}) and ideality factor (η_{ap}) are both temperature dependent [8, 11]. The above discussed contact behavior has been explained on the basis of an 'Analytical Potential Fluctuation Model' which assumes spatially inhomogeneous BHs at the interface [7, 27]. This model propagates that the distribution of the BHs is Gaussian in character with a mean value (ϕ_{bo}) and a standard deviation (σ_s), and is described as [9, 27].

$$P(\phi_{bo}) = \frac{1}{\sigma\sqrt{2\pi}}\exp\left(\frac{\phi_{bo} - \bar{\phi}_{bo}}{2\sigma_s}\right) \tag{4}$$

where $1/\sigma_s\sqrt{2\pi}$ is the normalization constant of the Gaussian barrier height distribution. The total current I(V) across a Schottky diode containing barrier inhomogeneities for any forward bias V is then given by,

$$I(V) = \int I(\phi_{bo}, V)P(\phi_{bo})d\phi \tag{5}$$

$$I(V) = A^{**}T^2\exp\left[\frac{-q}{KT}\left(\bar{\phi}_{bo} - \frac{\sigma_s^2 q}{2KT}\right)\right]\exp\left(\frac{q(V_s)}{KT}\right) \times \left[1 - \exp\left(\frac{-q(V_s)}{KT}\right)\right] \tag{6}$$

with,

$$I_s = AA^{**}T^2\exp\left(\frac{q\phi_{ap}}{KT}\right) \tag{7}$$

where η_{ap} and ϕ_{ap} are the apparent ideality factor and BH at zero bias, respectively, and the later is given by,

$$\sigma_{ap} = \bar{\phi}_{bo}(T=0) - \frac{\sigma_s^2 q}{2KT} \tag{8}$$

In the ideal case ($\eta = 1$), the expression is obtained as,

$$\left(\frac{1}{\eta_{ap}} - 1\right) = \rho_2 - \frac{q\rho_3}{KT} \tag{9}$$

The temperature dependence of σ_s is usually small and thus can be neglected [16]. However, it is assumed that σ_s and ϕ_{bo} are linearly bias dependent on Gaussian parameters such that $\bar{\phi}_b = \phi_{bo} + \rho_2 V$ and $\sigma_s = \sigma_{so} + \rho_3 V$, where ρ_2 and ρ_3 are the voltage coefficients that may depend on temperature and they quantify the voltage deformation of the BH distribution [16]. It is obvious that the decrease in zero-bias BH is caused by the existence of the GD, and the

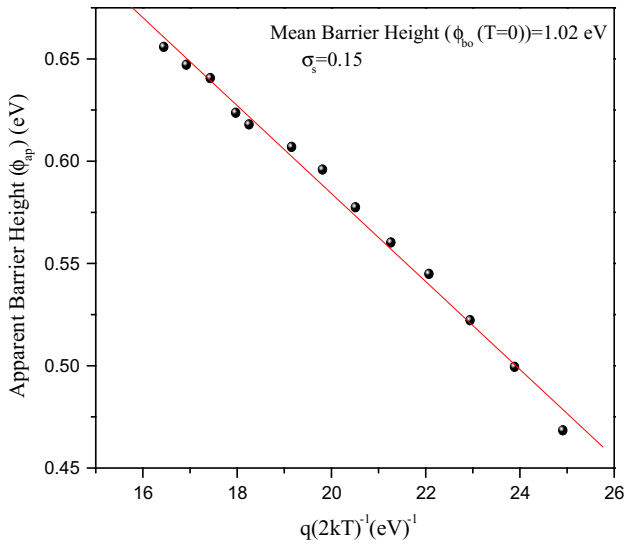

Fig. 4 Zero-bias apparent barrier height (ϕ_{ap}) versus q/2KT Al/p-CuInAlSe$_2$ Schottky diode as per to Gaussian distribution of the barrier heights

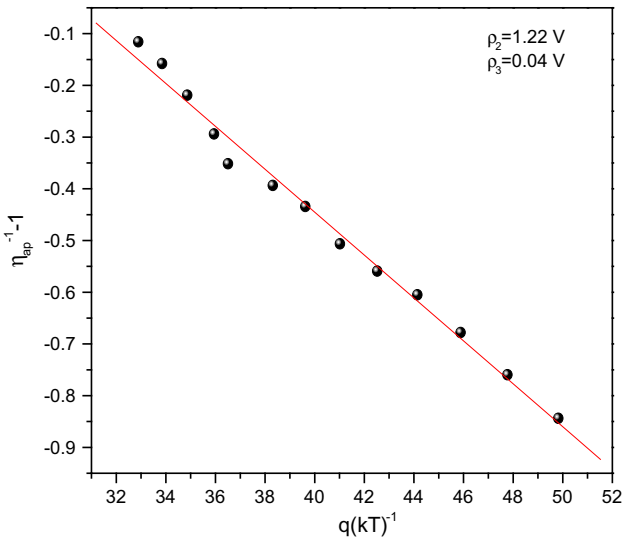

Fig. 5 Ideality factor (η_{ap}) versus q/KT plot of Al/p-CuInAlSe$_2$ Schottky diodes as per to Gaussian distribution of the barrier heights

extent of influence is determined by the standard deviation itself. Also, the effect is particularly significant at low temperatures. On the other hand, the abnormal increase in ideality factor occurs due to the variation of mean BH and standard deviation with bias, i.e., terms involving voltage coefficients ρ_2 and ρ_3.

The plot of ϕ_{ap} versus $q/2KT$ shown in Fig. 4 should be a straight line giving mean BH (ϕ_{bo}) and standard deviation (σ_s) as intercept and slope with values of 1.02 and 0.15 eV, respectively.

The solid line curves in Fig. 2 represent data generated from these parameters on their re-substitution to Eq. (8). This plot obeys TE model comprising GD of BHs given by the Eq. (8). By comparing ($\bar{\phi}_{bo}$) and (σ_s) parameters, it is seen that the standard deviation (a measure of the barrier inhomogeneity) is $\approx$15 % of the mean BH value. It has been noted that the lower value of σ_s corresponds to a more homogeneous character of BHs, the result thus indicates Al/p-CuInAlSe$_2$ Schottky diodes to possess inhomogeneous BH character, and these inhomogeneities as per the GD function represented in Eqs. (8) and (9). The cause of these deviations may be attributed to the variation in the composition of the interfacial oxide layer, nonuniformity of interfacial charges and variation of the interfacial oxide layer thickness, etc. [9, 14]. The temperature dependence of the ideality factor has been established to be controlled by lognormal function as represented by Eq. (9). The fitted ideality factor η plot shown in Fig. 5 is a straight line that gives voltage coefficients $\rho_2 = 1.22$ V and $\rho_3 = 0.04$ V from the intercept and slope. Furthermore, as can be seen from Fig. 5, the experimental results of η show good agreement with Eq. (9) for the same parameters. The linear

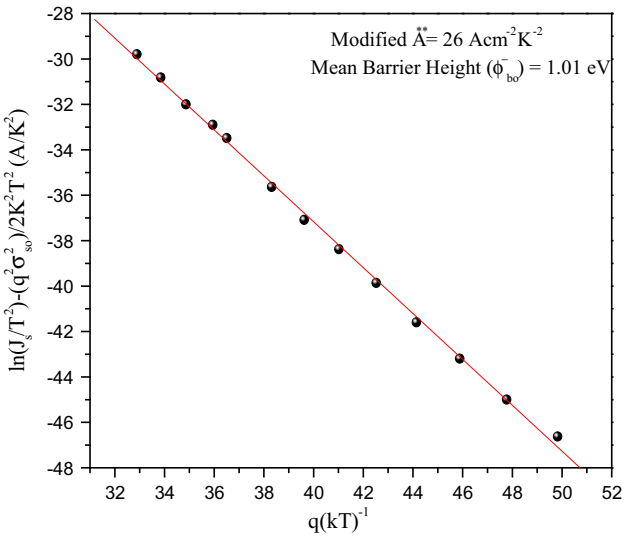

Fig. 6 Modified $\ln(J_s/T^2) - \left(q^2\sigma_s^2/2k^2T^2\right)$ versus q/kT plot for Al/p-CuInAlSe$_2$ Schottky diodes

plot of $(1/\eta_{ap} - 1)$ versus q/kT confirms that the ideality factor does indeed denote the voltage deformation of the GD of the BH. The continuous line in Fig. 2 represents data estimated with these parameters.

The Richardson plot presented at Fig. 3 according to Eq. (3) is now modified by combining Eqs. (8) and (9) we get,

$$\ln\left(\frac{J_s}{T^2}\right) - \left(\frac{q^2\sigma_s^2}{2k^2T^2}\right) = \ln(A^{**}) - \frac{q\overline{\phi_{bo}}}{kT} \qquad (10)$$

The modified $\ln(J_s/T^2) - (q^2\sigma_s^2/2k^2T^2)$ versus q/kT plot, given in Fig. 6, should also be a straight line with the

slope and the intercept at the ordinate yielding the mean BH ($\bar{\phi}_{bo}$) and A^{**}, respectively. The modified Richardson plot shows linearity according to the GD of BHs over the entire temperature range corresponding to single activation energy around ($\bar{\phi}_{bo}$) value. By the least squares linear fitting of the data, $\bar{\phi}_{bo} = 1.01$ eV it can be seen that the value of $\bar{\phi}_{bo}$ is in close agreement with the value of $\phi_{bo} = 1.02$ V obtained from the plot of ϕ_{ap} versus $q/2kT$ shown in Fig. 4, while modified Richardson constant $A^{**} = 26\ \mathrm{Acm^{-2}\ K^{-2}}$ is found to be in close agreement with the theoretical value of $A^{**} = 30\ \mathrm{Acm^{-2}\ K^{-2}}$. The modifications in the Richardson equations on adding the current components determined on the basis of barrier inhomogeneities caused barrier parameters $\bar{\phi}_{bo}$ and A^{**} to shift closer to their reported values, thus confirming the existence of 'barrier inhomogeneities.'

3.4 Capacitance–voltage–temperature (C–V–T) analysis

The C–V relationship for Schottky diode is [3, 4],

$$\frac{1}{C^2} = \left(\frac{2}{\varepsilon_s q N_a A^2}\right)\left(V_{bi} \frac{kT}{q} - V\right) \tag{11}$$

where ε_s is the permittivity of the semiconductor ($\varepsilon_s = 8.1\varepsilon_0$), V is the applied voltage. The x-intercept of the plot of ($1/C^2$) versus V gives V_0, and it is related to the built in potential V_{bi} by the equation:

$$V_{bi} = V_o + \frac{KT}{q} \tag{12}$$

where T is the absolute temperature. The BH is given by the equation,

$$\phi_{bo} = V_0 + \frac{KT}{q} + V_n \quad \text{or} \quad \phi_{bo} = V_{bi} + V_n \tag{13}$$

Here,

$$V_n = \left(\frac{kT}{q}\right) \ln\left(\frac{N_v}{N_A}\right) \tag{14}$$

The density of states in the conduction band edge is given by,

$$N_v = 2\left(\frac{2\pi m_e kT}{h^2}\right)^{3/2} \tag{15}$$

where m^* is hole effective mass ($m^* = 0.71\ m_o$) for $CuInSe_2$, h is the Planck's constant, and k is the Boltzmann constant. In order to access the doping concentration and BH reverse bias, C^{-2}–V characteristics of the Al/p-$CuInAlSe_2$ SBD in the temperature range of 233–353 K were obtained as shown in Fig. 7.

The junction capacitance is measured at a frequency of 1 MHz. The experimental C^{-2}–V plot measured at different temperatures has been found deviating from linearity. The nonlinearity of the curves indicates that the carrier concentration at the diode interface is not uniform. Further to that, the slope of the curves decreases with increasing bias, indicating an increase in N_A with increasing bias. This case indicates the presence of acceptor like deep traps (i.e., neutral when occupied, positively charged when empty) within the space charge region. The charge state of the acceptor like traps will depend on the position of the Fermi level.

The estimated Schottky BH of Al/p-$CuInAlSe_2$ Schottky diode is in the range of 0.81 eV at 233 K to 0.62 eV at 353 K, respectively (shown in Table 1). It is noted that the BH obtained from CV plot (ϕ_{CV}) increased with decrease in temperature. However, the BH obtained from the I–V curve decreases with decrease in temperature; this is attributed to inhomogeneous MS contacts. In the present case, the current transport at low temperatures has been dominated by current flowing through the patches of the lower BH with larger ideality factor as a result of the inhomogeneous MS contacts. The dominant BH obtained from the forward bias I–V characteristics will increase with the temperature due to barrier inhomogeneity in MS interface. This may be the reason of why the characteristics of the BH versus temperature plot obtained from the C–V measurements are completely opposite to those obtained from the I–V measurements [11]. Also, as clearly seen from Fig. 2, ϕ_{CV} increases with decreasing temperature as per the equation given as under:

$$\phi_{CV} = \phi_{CV}(T = 0K)\alpha T \tag{16}$$

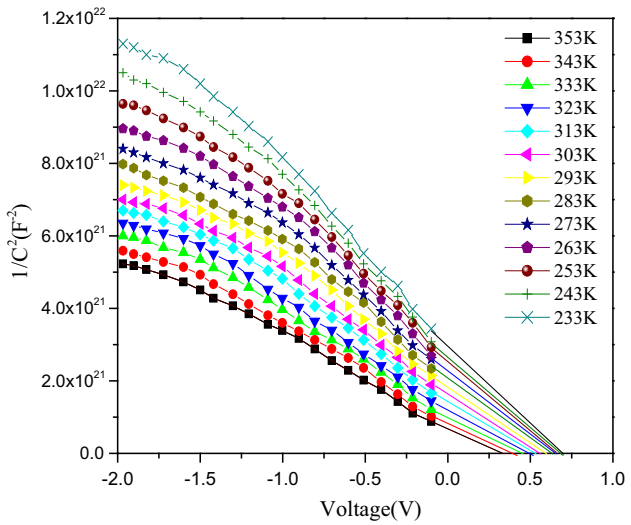

Fig. 7 Reverse bias C^{-2}–V characteristics of Al/p-$CuInAlSe_2$ SBD in the temperature range of 233–353 K

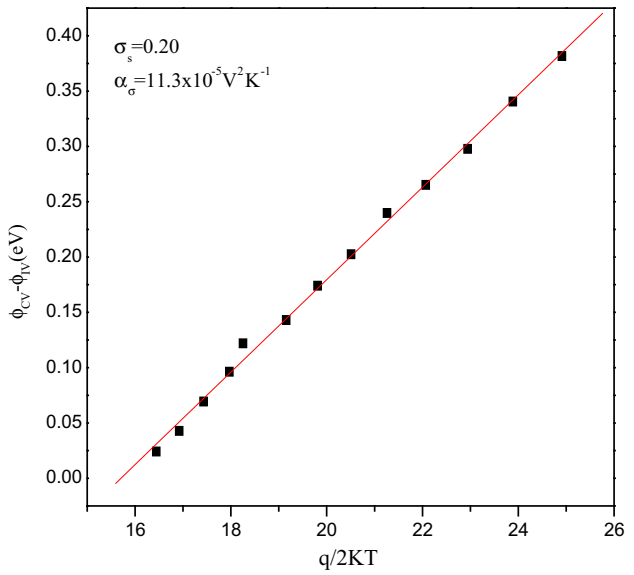

Fig. 8 Barrier height difference between values as derived from conventional evaluation of I–V and C–V data as a function of inverse temperature

where ϕ_{CV} ($T = 0$ K) is the BH extrapolated to zero temperature and α is the temperature coefficient of the BH. The linear fit of Eq. (16) to the experimental data in Fig. 2 yields ϕ_{CV} ($T = 0$ K) $= 1.1$ eV and $\alpha = -1.4 \times 10^{-3}$ eVK^{-1}.

Furthermore, it can be seen that the apparent BH from the experimental forward bias I–V plot is also related to the mean BH $\bar{\phi}_{IV} = \bar{\phi}_{CV}$ from the experimental reverse bias C^{-2}–V plot [8, 28]. The capacitance depends only on the mean band bending and is insensitive to the standard deviation (σ_s) of the barrier distribution [8, 28]. The relationship between ϕ_{IV} and ϕ_{CV} is given by [8, 28],

$$\phi_{CV} - \phi_{IV} = -\frac{q\sigma_s^2(T=0)}{2kT} + \frac{q\alpha_\sigma}{2k} \quad (17)$$

where α_σ is attributed to the temperature dependence of σ_s.

Figure 8 shows the experimental $(\phi_{CV}-\phi_{IV})$ versus $q/2kT$ plot according to Eq. (17). The plot should give a straight line with the slope providing the value of $\sigma_s = 0.20$ and y-axis intercept giving the value of $\alpha\sigma = 11.3 \times 10^{-5}$ V^{2}K^{-1}. The value of σ_s so obtained has been found in close agreement with the value of $\sigma_s = 0.15$ obtained from the plot of ϕ_{ap} versus $q/2kT$ shown in Fig. 4. This value of σ_s, however, is not small when compared with the mean BH value of 1.01 eV obtained from Fig. 4. Therefore, this may cause significantly large potential fluctuations particularly to the low temperature I–V data and could be responsible for the curved behavior of the conventional Richardson plot as shown in Fig. 3.

4 Conclusions

The effect of temperature on Al/p-CuInAlSe$_2$ Schottky diodes was investigated, wherein the nonideal I–V behavior of the Schottky diodes as displayed from its experimental data has been attributed to change in BH due to interface states defects, dislocations, surface states, series resistance, etc. The deviations from the experimental data have been explained on the basis of 'barrier height inhomogeneities' at the interface whose contribution when added confirmed the existence of TE phenomenon. The undertaken diodes were found to possess inhomogeneous BH character with a standard deviation of 15 % to the mean BH and were found to vary as per the GD function. The Richardson plot after inclusion of the current component generated on the basis of barrier inhomogeneities provided modified A^{**} and ϕ_{bo} values which are in close agreement with the reported ones. Existence of inhomogeneities has also been substantiated by the C–V analysis.

References

1. W.N. Shafarman, R. Klenk, B.E. McCandless, J. Appl. Phys. **79**, 7324 (1996)
2. T. Markvart, *Solar Electricity* (Wiley, England, 2000)
3. S.M. Sze, *Physics of Semiconductor Devices* (Wiley, New Jersey, 2007)
4. E.H. Rhoderick, R.H. Williams, *Metal–Semiconductor Contacts* (Clarendon Press, Oxford, 1978)
5. R.T. Tung, Mater. Sci. Eng.: R **35**, 131 (2001)
6. Z.J. Horvath, J. Mater. Sci. B **28**, 429 (1994)
7. Z.J. Horvath, Solid-State Electron. **39**, 176 (1996)
8. J.H. Werner, H.H. Güttler, J. Appl. Phys. **69**, 1522 (1991)
9. Y.P. Song, R.L. Van Meirhaeghe, W.F. Laflere, F. Cardon, Solid-State Electron. **29**, 633 (1986)
10. R.F. Schmitsdorf, T.U. Kampen, W. Möonch, Surf. Sci. **324**, 249 (1995)
11. J.P. Sullivan, R.T. Tung, M.R. Pinto, W.R. Graham, J. Appl. Phys. **70**, 7403 (1991)
12. R.T. Tung, Appl. Phys. Lett. **58**, 2821 (1991)
13. S. Chand, J. Kumar, J. Appl. Phys. **80**, 288 (1996)
14. W. Möonch, J. Vac. Sci. Technol., B **17**, 1867 (1999)
15. S.Y. Zhu, R.L. Van Meirhaeghe, Solid-State Electron. **44**, 663 (2000)
16. S. Chand, J. Kumar, Semicond. Sci. Technol. **10**, 1680 (1995)
17. U. Parihar et al., Mater. Chem. Phys. **139**, 270 (2013)
18. S. Chand, J. Kumar, J. Appl. Phys. **82**, 10 (1997)
19. S.K. Cheung, N.W. Cheung, Appl. Phys. Lett. **49**, 85 (1986)
20. Y.G. Chen, M. Ogura, H. Okushi, Appl. Phys. Lett. **82**, 4367 (2003)
21. M.B. Reddy, A.A. Kumar, Curr. Appl. Phys. **9**, 972 (2009)
22. F.A. Padovani, R. Stratton, Solid-State Electron. **9**, 695 (1996)
23. F.E. Cimili, M. Saglam, H. Efeoglu, A. Turut, Phys. B **404**, 344 (2009)
24. M. Soylu, B. Abay, Microelectron. Eng. **86**, 88 (2009)
25. S. Chand, J. Kumar, J. Appl. Phys. A **63**, 171 (1996)
26. N. Newman, M.V. Schilfgaarde, Phys. Rev. B **33**, 1146 (1986)
27. H. Norde, J. Appl. Phys. **50**, 5052 (1979)
28. H.H. Guttler, J.H. Werner, Appl. Phys. Lett. **56**, 1113 (1990)